crystals

MDPI

Review

Exploring Various Crystal and Molecular Structures of Gabapentin—A Review

Justyna Baranowska and Łukasz Szeleszczuk *

Department of Organic and Physical Chemistry, Faculty of Pharmacy, Medical University of Warsaw, Banacha 1 Street, 02-093 Warsaw, Poland; justyna.baranowska222@gmail.com
* Correspondence: lukasz.szeleszczuk@wum.edu.pl

Abstract: Novel antiepileptic drugs have been developed at an unparalleled rate during the past 15 years. Gabapentin (GBP), which was approved for the treatment of refractory localization-related epilepsies in the U.K. and Europe in 1993, was one of the first drugs to come out of this era. Since then, GBP has become well-known across the world, not only for its antiepileptic qualities but also for its effectiveness in the treatment of chronic pain disorders, particularly neuropathic pain. In this review, the crystal structures of GBP and GBP-related compounds have been analyzed and compared. Particular attention has been paid to the polymorphism of GBP and its hydrates, their thermodynamic stability, and conformational differences. In addition, the puckering parameters for the cyclohexane ring of a total of 118 molecules of GBP found in the analyzed crystal structures have been calculated and analyzed. The results of recent high-pressure crystallization studies and quantum chemical calculations indicate that the entire landscape of GBP has not been revealed yet.

Keywords: gabapentin; GABA; puckering; API; crystal structure

Citation: Baranowska, J.; Szeleszczuk, Ł. Exploring Various Crystal and Molecular Structures of Gabapentin—A Review. *Crystals* **2024**, *14*, 257. https://doi.org/10.3390/cryst14030257

Academic Editors: Matteo Mori and Fiorella Meneghetti

Received: 15 February 2024
Revised: 28 February 2024
Accepted: 2 March 2024
Published: 6 March 2024

1. Introduction

Gabapentin (GBP) is a common name for 1-(aminomethyl)cyclohexaneacetic acid ($C_9H_{17}NO_2$, CAS Registry No. 60142-96-3), a GABA (γ-aminobutyric acid) derivative (Figure 1) and a popular active pharmaceutical ingredient (API) [1,2]. It has a molecular weight of 171.34 and two pKa values of 3.68 and 10.70 [3,4]. Therefore, at physiological pH, GBP exists in the form of a zwitterion. It was originally developed in 1977 in an effort to create a structural analog of gamma-aminobutyric acid (GABA) with higher lipophilicity than the original neurotransmitter, thus enhancing its ability to enter the central nervous system [5].

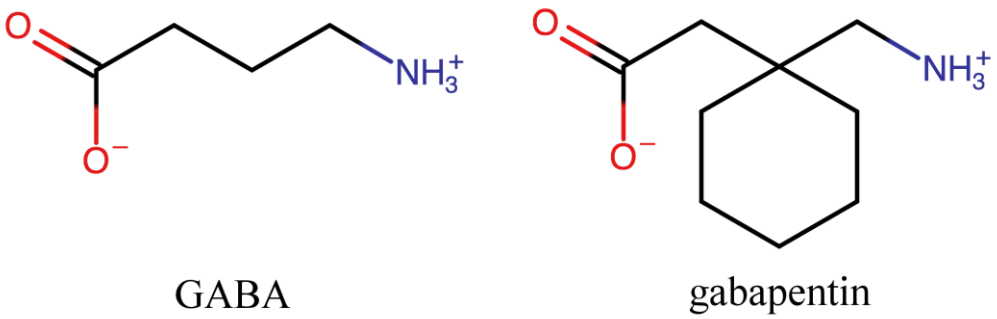

Figure 1. Chemical structure of GABA and its derivative, gabapentin (GBP).

Gabapentin is an antiepileptic drug that is considered a first-line treatment for the management of neuropathic pain. GBP is also approved for the treatment of focal seizures. However, it is ineffective in treating generalized epilepsy [4,6,7]. Aside from neuropathic pain, off-label use in primary care is very common. These include the treatment of a wide

range of conditions such as bipolar disorder, complex regional pain syndrome, attention deficit disorder, restless legs syndrome, and periodic limb movement, alongside sleep disorders, headaches, alcohol withdrawal syndrome, chronic back pain, fibromyalgia, visceral pain, and acute postoperative pain [5].

Despite its quite simple formula, it took almost 25 years from the first synthesis to the crystal structure determination of GBP in 2001. However, during the subsequent 23 years, multiple forms of this API have been successfully obtained, and their crystal structures have been solved. GBP, due to its relatively short half-life, is usually administered three times daily. Therefore, exploration of the solid landscape of this drug has been, at least partially, motivated by the desire to improve its pharmacokinetic properties.

This article reviews the solid forms of gabapentin, including its polymorphs, solvates, salts, and cocrystals as well as even more complexed systems. It starts with a summary of the pharmacological properties of this API, followed by a detailed look at 46 structures in which GBP is present. Finally, the chosen molecular properties of GBP present in those structures are presented and compared.

2. Materials and Methods

Crystal structures of systems containing GBP were downloaded using ConQuest version 2022.3.0 [8]. An additional check was performed on 22 January 2024 using the online version of the CCDC Access Structure application [9] to include the most recently deposited structures. BIOVIA Materials Studio 2020 Visualizer [10] was used for visualization purposes. Shinya Fushinobu Cremer-Pople parameter calculator [11] was used to determine the puckering parameters.

3. Pharmaceutical Properties of GBP

3.1. Pharmacological Properties

3.1.1. Mechanism of Action

Despite multiple extensive studies, the exact mechanisms of action of GPB remain unknown [4,12,13]. It has been proven in vivo that GBP does not bind to GABA receptors [12] despite its structural similarity to this neurotransmitter. However, it displays a high affinity for the α2δ-1 subunit of voltage-gated calcium channels (VGCCs) [12,14]. Therefore, it is commonly considered that GBP's analgesic effects are due to the suppression of calcium currents by binding to the α2δ-1 subunit, resulting in reduced postsynaptic excitability [14]. This assumption, however, is inaccurate because GBP has not been demonstrated to reliably inhibit Ca^{2+} currents [12]. Despite this, GBP is helpful in the therapy of neuropathic pain, which is achieved by inhibiting the release of different neurotransmitters at neural synapses [4,12].

3.1.2. Pharmacokinetics

GBP is absorbed in the small intestine. The only factor that affects GBP absorption is L-type amino acid transporter (LAT), which is easily saturable and causes dose-dependent pharmacokinetics [15]. More specifically, LAT-1 actively carries GBP across the blood–brain barrier. The area under the plasma concentration–time curve (AUC) does not rise in proportion to an increase in GBP dosage. This API has no affinity for plasma proteins. Peak levels of cerebrospinal fluid require a median of 8 h to reach, which is a considerably longer time than peak plasma levels. GBP does not influence spinal neurotransmitter concentrations of glutamate, norepinephrine, substance P, or calcitonin gene-related peptide. The volume of distribution of GPB is 0.8 L/kg, and it is highly water soluble. Although GBP is not metabolized by the liver and does not impact the major isoenzymes of the cytochrome P450 system, case studies have reported drug-induced hepatotoxicity [16]. Elimination is mostly performed by the kidney and is proportional to creatinine clearance. Adverse reactions may arise from accumulation, leading to renal failure [5].

3.2. Medical Uses

3.2.1. Neuropathic Pain

Gabapentin is effective in the therapy of postherpetic neuralgia and diabetic neuropathy; however, there is limited evidence in other types of neuropathic pain [12]. Numerous international and regional professional organizations have released clinical practice guidelines recommending gabapentinoids, including GBP, as first-line therapy. For neuropathic pain other than trigeminal neuralgia, the National Institute of Clinical Excellence (NICE) guidelines prescribe gabapentin, pregabalin, amitriptyline, or duloxetine as the first line of treatment [12].

3.2.2. Seizures

GBP is a second-generation antiseizure drug, which has been shown to be effective as an addition to other anticonvulsants in the treatment of partial seizures and generalized tonic–clonic seizures in children over the age of 12 [4]. In three extensive multicenter, double-blind, randomized dosage, controlled studies, 649 patients were involved, and the results showed that gabapentin, when used alone, was both safe and effective in treating partial seizures [4]. Gabapentin is ineffective in absence seizures [17].

3.2.3. Drug Dependence

GBP is one of several anticonvulsants that have been studied for the treatment of drug abuse disorders. Their effectiveness in treating cocaine addiction has been shown to be ineffective [18], and while the evidence for treating alcohol and cannabis addiction is promising, it is either not sufficient or of low quality [19,20].

3.2.4. Restless Legs Syndrome

In a comparative analysis of suggested therapies for restless legs syndrome, GBP was found to be linked to comparable reductions in the International Restless Legs Syndrome, receiving a similar score as dopamine agonists [21]. On the other hand, a higher improvement in the Periodic Limb Movement Index was linked to dopamine agonists [21]. Regarding the Clinical Practice Guideline of the American Academy of Sleep Medicine, GBP has been accepted as a possible therapeutic choice for this syndrome [22]. However, only GBP enacarbil is approved in the United States for the treatment of this illness [5].

3.3. Dosages

Gabapentin is well tolerated at doses ranging from 800 to 1800 mg/day [13]. However, according to the medication package insert of some drugs, patients may be treated with doses as high as 3600 mg/day [4].

3.3.1. Dosages in Epilepsy

Gabapentin oral doses are administered three times daily due to its relatively short half-life [4]. For adults and children over 12 years old with epilepsy, dosages up to 2400 mg per day are advised. Rapid titration can be performed with doses of 300 mg once daily on the first day, which are usually at bedtime to avoid side effects like sedation and drowsiness, 300 mg twice daily on the second day, and 300 mg three times daily on the third day. If efficacy is not obtained at this dose, the dosage may be increased further.

3.3.2. Dosages in Neuropathic Pain

The starting dose for the treatment of neuropathic pain is 300 mg three times per day, with escalation if necessary to a daily maximum of 3600 mg, although there have been reports of doses up to 4200 mg. The beneficial effects of gabapentin in neuropathic pain and in a variety of other chronic pain disorders are supported by evidence from both animal and human trials [4].

3.4. Side Effects

Dizziness, sedation, somnolence, peripheral edema, and weight gain are the most frequent adverse effects; these side effects appear to be dose-dependent. GBP's relative lack of interactions and severe side effects make it a desirable therapeutic alternative [5].

4. Overview of the Crystal Structures of Systems Containing GBP

As stated in the Introduction, chronologically, the first determined were the structures of anhydrous GBP (QIMKIG) and its monohydrate (QIMKOM). However, during subsequent years of crystallographic studies, multiple new forms of GBP have been successfully obtained, and their structures have been determined.

The table below (Table 1) presents the crystal structures of systems containing GBP. To facilitate the analysis, they have been grouped into several categories. The first one includes the polymorphic forms of anhydrous GBP, which have been described in detail below in Table 2.

The second group consists of hydrates of GBP in the zwitterionic form [23] as well as in the form of hydrochloride. This group has also been described below in Table 3.

The third group includes salts of GBP. So far, in all the deposited structures of salts, GBP exists solely as a cation, despite its ability to form anions due to the presence of a carboxyl group. The variety of anions found in this group is large and includes both simple organic anions such as oxalate, picrate, or salicylate as well as inorganic ions such as $[AuCl_4]$, nitrate, or dihydrophosphate [24].

The next group of structures includes cocrystals and inclusion complexes with macrocycles, in which GBP exists as a guest.

Due to the presence of an ionized carboxyl group, GBP can serve as a Lewis base [25]. Throughout the years, multiple systems have been obtained in which GBP exists as a ligand. This includes complexes with both commonly encountered metals such as Cu [26], Zn [27], and Mn and also with more unusual ones such as Er or Y. Interestingly, in one of those structures, VIXQAW, there are 16 GBP ligands in the asymmetric unit.

While in most structures, GBP exists either as zwitterion or cation, in one of the structures, FOXNUC, presenting gabapentin hydrogenbis(4-hydroxybenzoate), a quite unusual form of GBP can be observed, which from the formal point of view can be described as GBP_2H^+ (Figure 2).

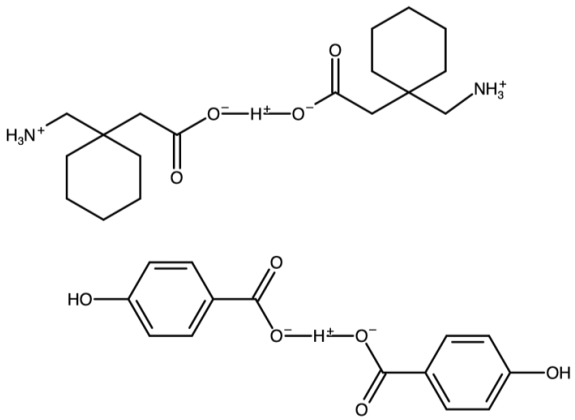

Figure 2. Chemical structure of gabapentin hydrogenbis(4-hydroxybenzoate), present in FOXNUC.

Table 1. Crystal structures of systems including GBP.

Chemical Name	CCDC Refcode	Molecular Structure	Reference and Year of Depositon	Methods of Physicochemical Analysis Other than SCXRD
Gabapentin polymorphs				
Gabapentin α (II) polymorph	QIMKIG	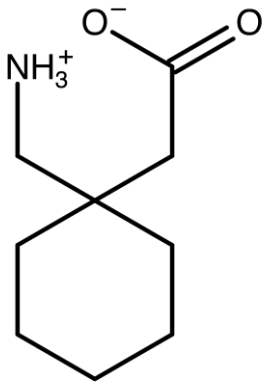	[28] 2001	
	QIMKIG01		[29] 2004	^{1}H IS NMR
	QIMKIG06		[30] 2017	PXRD TGA Optical microscopy GC Solubility measurements MD
Gabapentin β (IV) polymorph	QIMKIG02		[31] 2008	
	QIMKIG04		[32] 2009	PXRD DSC Melting point HSM Stability at 50 and 100% RH
Gabapentin γ (III) polymorph I	QIMKIG03		[31] 2008	
	QIMKIG05		[32] 2009	PXRD DSC Melting point HSM Stability at 50 and 100% RH
Gabapentin hydrates				

Table 1. *Cont.*

Chemical Name	CCDC Refcode	Molecular Structure	Reference and Year of Depositon	Methods of Physicochemical Analysis Other than SCXRD
Gabapentin monohydrate	QIMKOM (I) polymorph	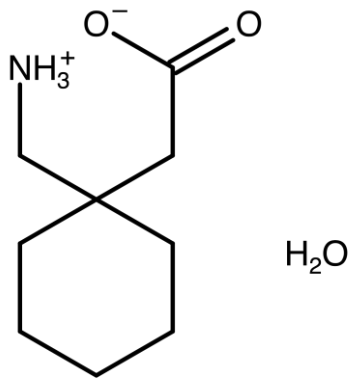	[28] 2001	
	QIMKOM01 (I) polymorph		[33] 2010	
	QIMKOM03 (I) polymorph		[30] 2017	PXRD TGA Optical microscopy GC Solubility measurement MD
	QIMKOM02 (II) polymorph		[33] 2010	
	QIMKOM04 (II) polymorph		[34] 2022	PXRD DSC TGA FTIR RM DVS SEM
Gabapentin heptahydrate	YUZTET	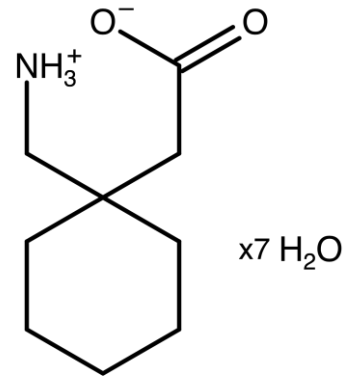	[35] 2010	

Table 1. *Cont.*

Chemical Name	CCDC Refcode	Molecular Structure	Reference and Year of Depositon	Methods of Physicochemical Analysis Other than SCXRD
Gabapentin hydrochloride hemihydrate	AWUWIY *C 2/c* polymorph	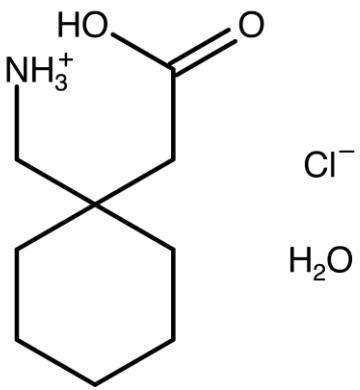	[29] 2004	^{1}H IS NMR
	AWUWIY01 *I 2/a* polymorph		[36] 2010	
	AWUWIY02 *C 2/c* polymorph		[37] 2016	PXRD DSC
Gabapentin salts				
Gabapentin with terephthalic acid	AVILOH	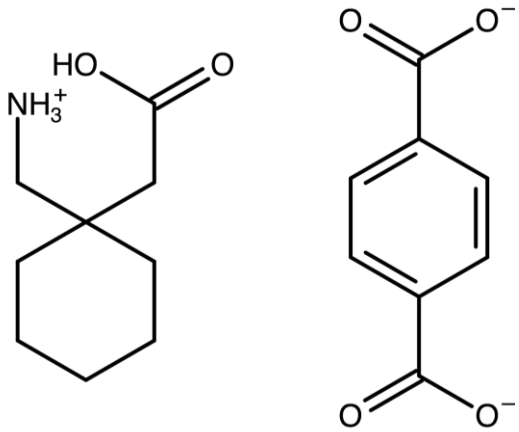	[38] 2011	PXRD HSM DSC TGA FTIR

Table 1. *Cont.*

Chemical Name	CCDC Refcode	Molecular Structure	Reference and Year of Depositon	Methods of Physicochemical Analysis Other than SCXRD
Gabapentin hemikis(oxalate)	SOCYUF	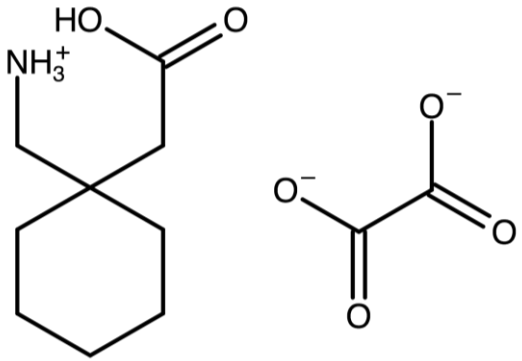	[39] 2008	PXRD HSM DSC
Gabapentinium picrate	LORQIT	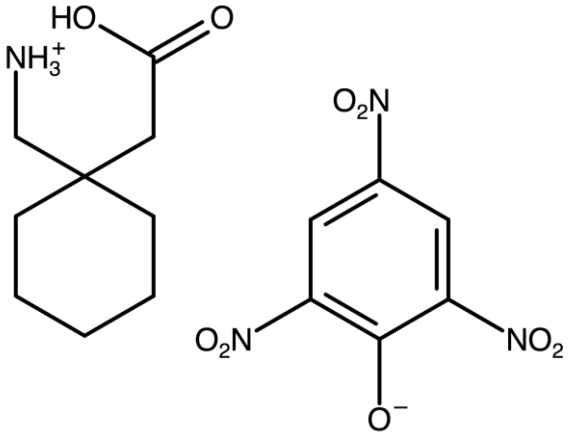	[40] 2009	

Table 1. *Cont.*

Chemical Name	CCDC Refcode	Molecular Structure	Reference and Year of Depositon	Methods of Physicochemical Analysis Other than SCXRD
Gabapentin–[AuCl4]−salt	AVAVAV	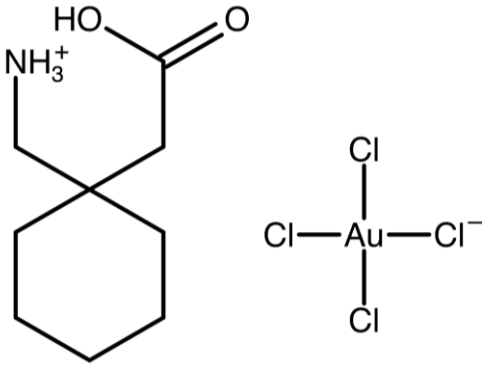	[41] 2011	^{1}H IS NMR
Gabapentin 1-hydroxy-2-naphthoate	FOXPEO	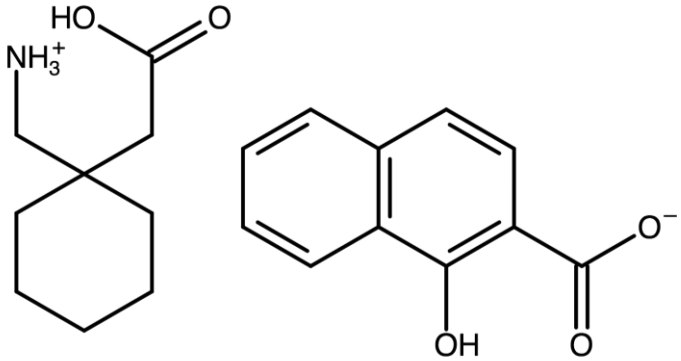	[42] 2010	PXRD DSC RM IR

Table 1. *Cont.*

Chemical Name	CCDC Refcode	Molecular Structure	Reference and Year of Depositon	Methods of Physicochemical Analysis Other than SCXRD
Gabapentin RS-mandelate	FOXPOY	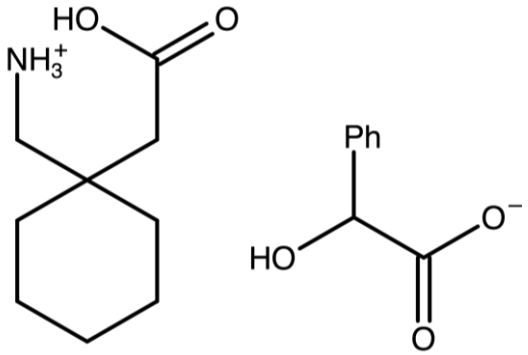	[42] 2010	PXRD DSC RM IR
Gabapentin salicylate	FOXPAK	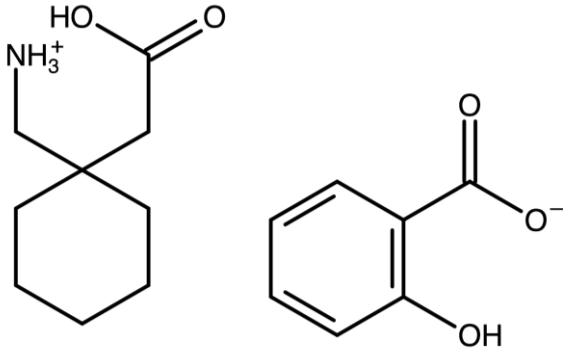	[42] 2010	PXRD DSC RM IR

Table 1. *Cont.*

Chemical Name	CCDC Refcode	Molecular Structure	Reference and Year of Depositon	Methods of Physicochemical Analysis Other than SCXRD
Gabapentin nitrate	IKATIY	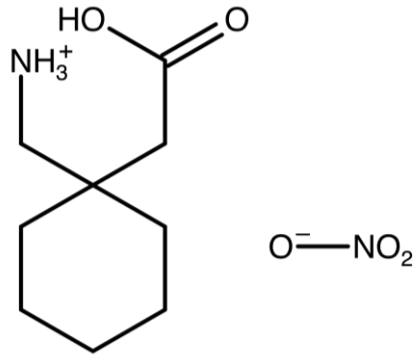	[43] 2011	
Gabapentinium dihydrogen phosphate	NUPXAY	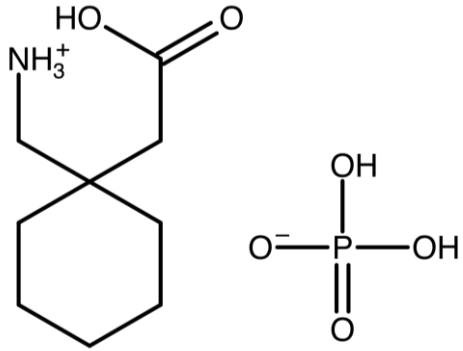	[44] 2010	
		Cocrystals and host-guest complexes		

Table 1. *Cont.*

Chemical Name	CCDC Refcode	Molecular Structure	Reference and Year of Depositon	Methods of Physicochemical Analysis Other than SCXRD
Gabapentin with trimesic acid	AVILUN	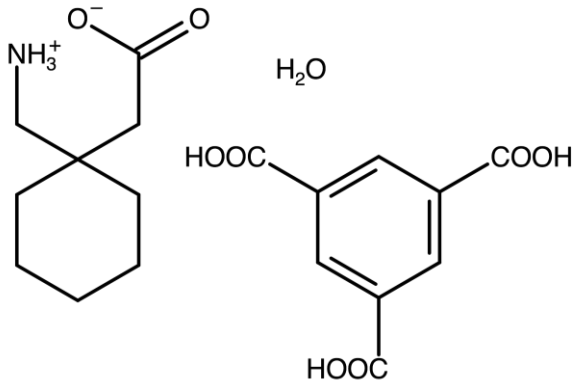	[38] 2011	PXRD HSM DSC TGA FTIR
Gabapentin 4-aminobenzoic acid	DESNOI	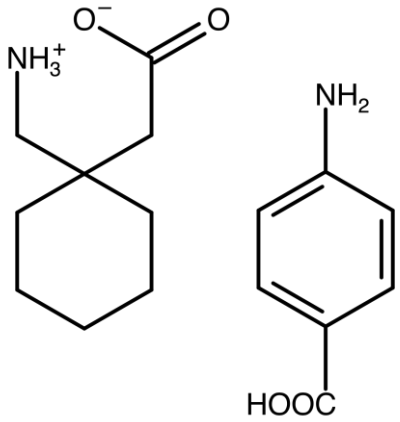	[34] 2022	PXRD DSC TGA FTIR RM DVS SEM

Table 1. *Cont.*

Chemical Name	CCDC Refcode	Molecular Structure	Reference and Year of Depositon	Methods of Physicochemical Analysis Other than SCXRD
Gabapentin 3-hydroxybenzoic acid	FOXNOW	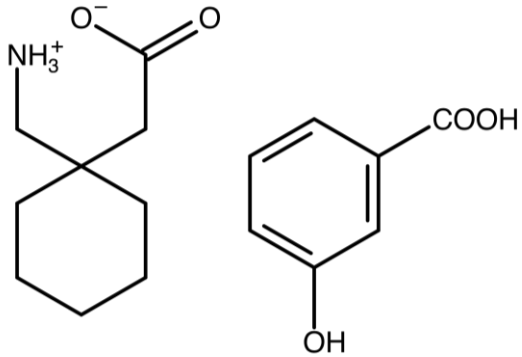	[42] 2010	PXRD DSC HPLC RM IR
Pyrogallol[4]arene with gabapentin	ELUNOP	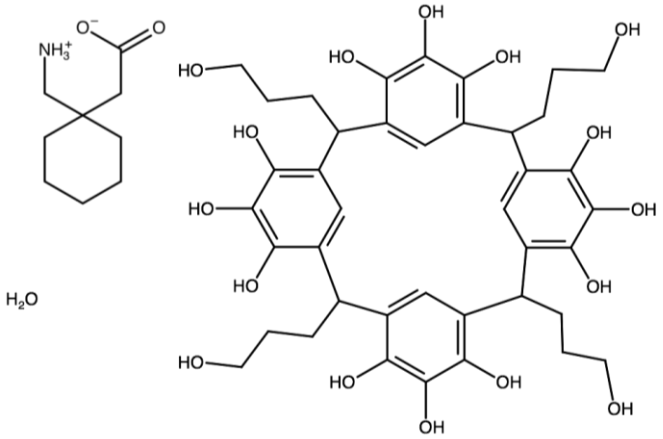	[45] 2011	

Table 1. *Cont.*

Chemical Name	CCDC Refcode	Molecular Structure	Reference and Year of Depositon	Methods of Physicochemical Analysis Other than SCXRD
C-butylpyrogallol[4]arene bis(gabapentin)	ANISAS	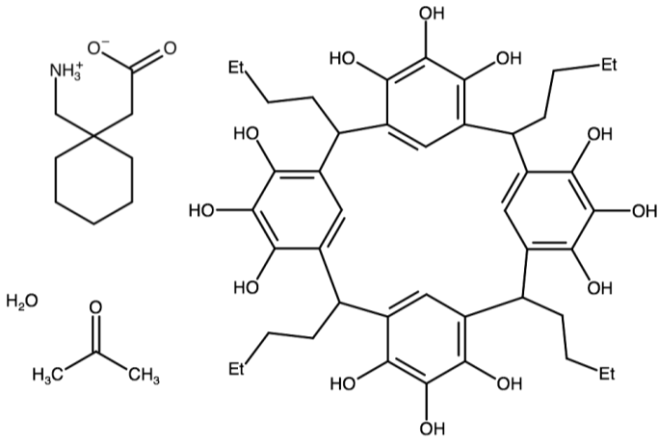	[45] 2011	
bis(C-butylpyrogallol[4]arene) tetrakis(gabapentin)	ANISEW	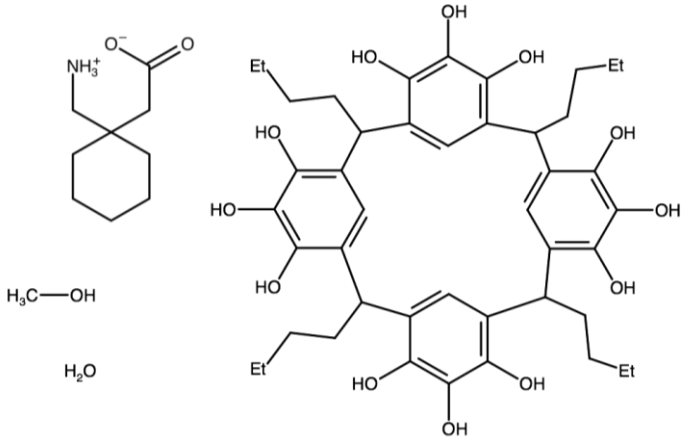	[45] 2011	

Table 1. *Cont.*

Chemical Name	CCDC Refcode	Molecular Structure	Reference and Year of Depositon	Methods of Physicochemical Analysis Other than SCXRD
[1-(azaniumylmethyl)cyclohexyl]acetate 2,8,14,20-tetrapropylpentacyclo[19.3.1.1^{3,7}.1^{9,13}.1^{15,19}]octacosa-1(25),3(28),4,6,9(27),10,12,15(26),16,18,21,23-dodecaene-4,5,6,10,11,12,16,17,18,22,23,24-dodecol 1,2-dichlorobenzene	EFIVIB	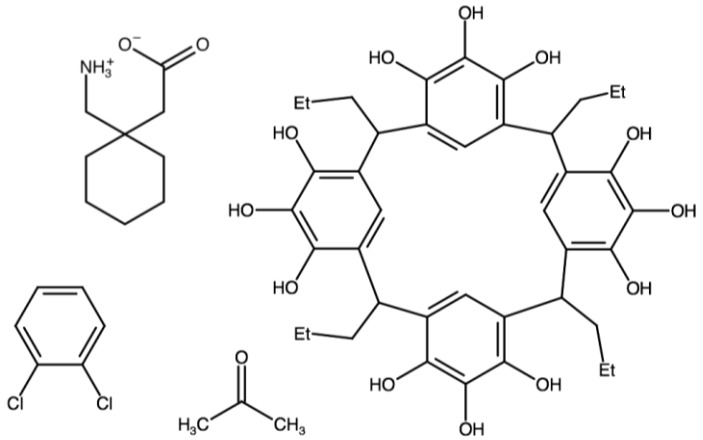	[46] 2019	
2,8,14,20-tetrahexyl-4,6,10,12,16,18,22,24-octahydroxycalix(4)arene (1-(aminomethyl)cyclohexyl)acetic acid methanol solvate monohydrate	SESKEI	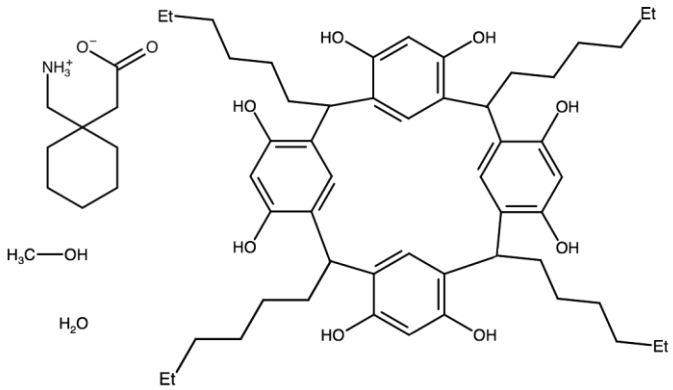	[47] 2013	PXRD

Table 1. *Cont.*

Chemical Name	CCDC Refcode	Molecular Structure	Reference and Year of Depositon	Methods of Physicochemical Analysis Other than SCXRD
		Complexes with metals		
tetrakis(μ2-[1-(ammoniomethyl)cyclohexyl]acetato)-bis([1-(ammoniomethyl)cyclohexyl]acetato)-diaqua-dichloro-di-erbium tetrachloride octahydrate	VIXBUB	$[Er_2GBP_6(H_2O)_2Cl_2]Cl_4 \cdot 8H_2O$	[48] 2014	PXRD DSC TGA HPLC ^{1}H IS NMR
octakis(μ2-[1-(ammoniomethyl)cyclohexyl]acetato)-bis([1-(ammoniomethyl)cyclohexyl]acetato)-tetraaqua-tri-lanthanum nonachloride dodecahydrate	VIXCAI	$[La_3GBP_{10}(H_2O)_4]Cl_9 \cdot 12H_2O$	[48] 2014	PXRD DSC TGA HPLC ^{1}H IS NMR
bis([1-(ammoniomethyl)-cyclohexyl]acetato)-diaqua-dichloro-manganese(ii)	VIXCEM	$[MnGBP_2(H_2O)_2Cl_2]$	[48] 2014	PXRD DSC TGA HPLC ^{1}H IS NMR
bis([1-(ammoniomethyl)-cyclohexyl]acetato)-diaqua-dichloro-manganese(ii)	VIXCEM01	$[MnGBP_2(H_2O)_2Cl_2]$	[48] 2014	PXRD DSC TGA HPLC ^{1}H IS NMR
bis(μ2-[1-(ammoniomethyl)-cyclohexyl]acetato)-tetrakis(μ2-chloro)-bis([1-(ammoniomethyl)-cyclohexyl]acetato)-diaqua-dichloro-tri-manganese	VIXCIQ	$[Mn_3GBP_4(H_2O)_2Cl_6]$	[48] 2014	PXRD DSC TGA HPLC ^{1}H IS NMR
tetrakis(μ2-[1-(ammoniomethyl)-cyclohexyl]acetato)-bis([1-(ammoniomethyl)cyclohexyl]acetato)-diaqua-dichloro-di-neodymium tetrachloride octahydrate	VIXCUC	$[Nd_2GBP_6(H_2O)_2Cl_2]Cl_4 \cdot 8H_2O$	[48] 2014	PXRD DSC TGA HPLC ^{1}H IS NMR

Table 1. *Cont.*

Chemical Name	CCDC Refcode	Molecular Structure	Reference and Year of Depositon	Methods of Physicochemical Analysis Other than SCXRD
tetrakis(μ2-[1-(ammoniomethyl)-cyclohexyl]acetato)-bis([1-(ammoniomethyl)cyclohexyl]acetato)-diaqua-dichloro-di-yttrium tetrachloride octahydrate	VIXDAJ	$[Y_2GBP_6(H_2O)_2Cl_2]Cl_2 \cdot 8H_2O$	[48] 2014	PXRD DSC TGA HPLC ^{1}H IS NMR
catena-[pentakis(μ2-[1-(ammoniomethyl)-cyclohexyl]acetato-O,O′)-tris(μ2-[1-(ammoniomethyl)cyclohexyl]acetato-O,O,O′)-penta-aqua-tri-yttrium nonachloride decahydrate]	VIXDEN	$[Y_3GBP_8(H_2O)_5]Cl_9 \cdot 10H_2O$	[48] 2014	PXRD DSC TGA HPLC ^{1}H IS NMR
tetradecakis(μ2-[1-(ammoniomethyl)-cyclohexyl]acetato)-bis([1-(ammoniomethyl)cyclohexyl]acetato)-decaaqua-tetrachloro-hexa-cerium tetradecachloride icosahydrate	VIXQAW	$[Ce_6GBP_{16}(H_2O)_{10}Cl_4]Cl_{14} \cdot 20H_2O$	[48] 2014	PXRD DSC TGA HPLC ^{1}H IS NMR
octakis(μ2-[1-(ammoniomethyl)-cyclohexyl]acetato)-bis([1-(ammoniomethyl)cyclohexyl]acetato)-tetraaqua-tri-cerium nonachloride dodecahydrate	VIXQEA	$[Ce_3GBP_{10}(H_2O)_4]Cl_9 \cdot 12H_2O$	[48] 2014	PXRD DSC TGA HPLC ^{1}H IS NMR
bis(μ3-hydroxo)-tetrakis(μ2-[1-(carboxylatomethyl)cyclohexyl]-methanaminium)-tetraaqua-bis(nitrato)-tetra-zinc(ii) tetranitrate	UQUMOJ	$[Zn_4(OH)_2(NO_3)_2(C_9H_{17}\text{-}NO_2)_4(H_2O)_4](NO_3)_4$	[49] 2011	
Dichloro-bis(1-(ammoniomethyl)-cyclohexane acetate)-zinc(ii)	DOBBIG	$[ZnCl_2(GBP)_2]$	[50] 2008	PXDR
Dichloro-bis(1-(ammoniomethyl)-cyclohexane acetate)-copper(ii)	DOBBOM	$[CuCl_2(GBP)_2]$	[50] 2008	PXDR
(gabapentin)-penta-aqua-nickel(ii) sulfate monohydrate	JALXEC	$[Ni(H_2O)_5(GBP)]SO_4 \cdot H_2O$	[51] 2014	

Table 1. *Cont.*

Chemical Name	CCDC Refcode	Molecular Structure	Reference and Year of Depositon	Methods of Physicochemical Analysis Other than SCXRD
bis{[1-(aminomethyl)cyclohex-yl]acetato}-bis{[1-(aminome-thyl)cyclohexyl]acetic acid}-diaqua-cobalt(ii)	JALXAY	$[Co(H_2O)_2(GBP)_4]$	[51] 2014	
		Other		
Gabapentin hydrogenbis(4-hydroxybenzoate)	FOXNUC	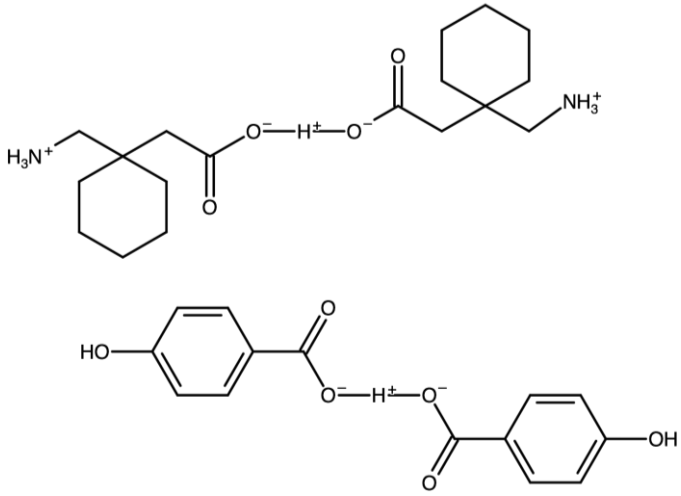	[42] 2010	PXDR DSC HPLC RM IR

The abbreviations used above for analytical methods stand for: SCXRD—Single Crystal X-ray Diffraction; PXDR—Powder X-Ray Diffraction; TGA—Thermogravimetric Analysis; MD—Molecular Dynamic Simulations; DSC—Differential Scanning Calorimetry; HSM—Hot-stage Microscopy; GC—Gas Chromatography; FTIR—Fourier Transform Infrared Spectroscopy; HPLC—High-Performance Liquid Chromatography; RM—Raman Spectroscopy; IR—Infrared Spectroscopy; IS NMR—Solution NMR; DVS—Dynamic Water Vapor Sorption Isotherm; SEM—Microscopic Analysis with Scanning Electron Microscope.

Table 2. Crystal structures of polymorphic forms of anhydrous GBP.

Refcode	Polymorph	Space Group	a [Å]	b [Å]	c [Å]	α [°]	β [°]	γ [°]	V [Å^3]	Z	Z′
QIMKIG	α	14 $P2_1/c$	5.88	6.92	22.26	90.00	90.08	90.00	905.17	4	1
QIMKIG01	α	14 $P2_1/c$	5.90	6.92	22.48	90.00	90.06	90.00	918.09	4	1
QIMKIG06	α	14 $P2_1/c$	5.90	6.92	22.46	90.00	90.00 *	90.00	917.68	4	1
QIMKIG02	β	14 $P2_1/c$	14.54	6.63	9.83	90.00	105.92	90.00	911.91	4	1
QIMKIG04	β	14 $P2_1/c$	14.74	6.67	9.89	90.00	106.09	90.00	933.39	4	1
QIMKIG03	γ	15 $C2/c$	30.55	5.93	10.88	90.00	108.32	90.00	1870.58	8	1
QIMKIG05	γ	15 $C2/c$	30.58	5.93	10.92	90.00	108.31	90.00	1879.87	8	1

* The β angle is not strictly 90° but 90.00(3)°.

Table 3. Crystal structures of hydrates of GBP.

	Refcode	Polymorph	Space Group	a [Å]	b [Å]	c [Å]	α [°]	β [°]	γ [°]	V [Å^3]	Z	Z′
Monohydrates	QIMKOM	I	14 $P2_1/c$	14.57	9.22	7.65	90.00	93.38	90.00	1025.19	4	1
	QIMKOM01	I	14 $P2_1/c$	14.63	9.31	7.67	90.00	93.16	90.00	1043.11	4	1
	QIMKOM03	I	14 $P2_1/c$	14.63	9.30	7.65	90.00	93.11	90.00	1039.08	4	1
	QIMKOM04	II	61 $P\,b\,c\,a$	9.22	7.64	29.00	90.00	90.00	90.00	2040.90	8	1
	QIMKOM02	II	61 $P\,b\,c\,a$	29.14	9.30	7.66	90.00	90.00	90.00	2074.35	8	1
Heptahydrate	YUZTET		2 P-1	6.80	7.32	15.84	86.30	78.92	72.71	737.49	2	1

5. Polymorphism of Anhydrous and Hydrated Forms of GBP

There are several forms of GBP that have been the subject of numerous research studies, patent applications, and grants of patents. Both the anhydrous and hydrated forms are affected by polymorphism.

5.1. Polymorhphism of Anhydrous GBP—Structures QIMKIGXX

Anhydrous GBP exists in three different forms—α, γ, and β, sometimes also described as II, III, and IV (Table 2). The lack of form I in this group is a result of the convention that was established in the first work presenting the crystal structure of GBP [28]. According to it, anhydrous GBP is form II, while the monohydrate is form I.

Chronologically, the first described one (2001) was the α polymorph present in the structures QIMKIG, QIMKIG01, and QIMKIG06. Subsequently, β-gabapentin was first obtained by Pesachovich et al. (2001) [52], while γ-gabapentin was discovered by Satyanarayana et al. (2004) [53]. However, the crystal structures of both the β and γ polymorphs were first solved by Reece and Levendis (2008) [31].

The α and β polymorphs crystallize in the same space group, $P2_1/c$ with Z = 4, whereas the space group of γ is $C2/c$ and Z = 8. In all forms, there is only one molecule of GBP in the asymmetric unit. The crystal structures are stabilized by dense networks of hydrogen bonds formed between the NH_3^+ and COO^- groups of nearby molecules that exist in all three polymorphs of GBP (Figure 3). In addition, β-gabapentin possesses an additional intramolecular hydrogen bond formed between the same groups. The GBP crystallizes as a zwitterion in all the known anhydrous forms.

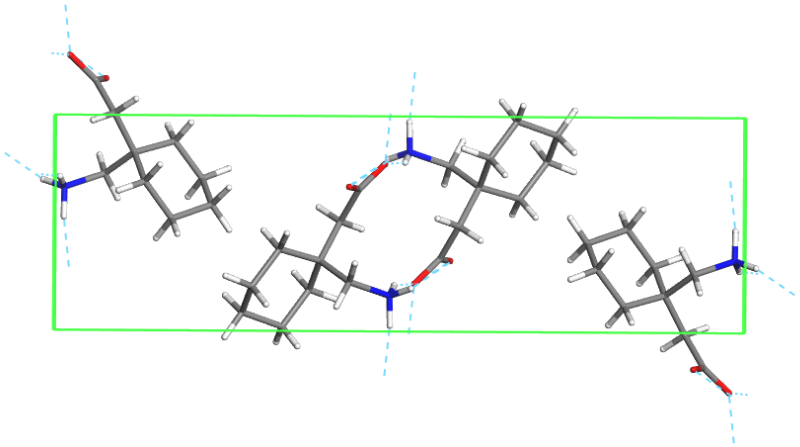

α-gabapentin

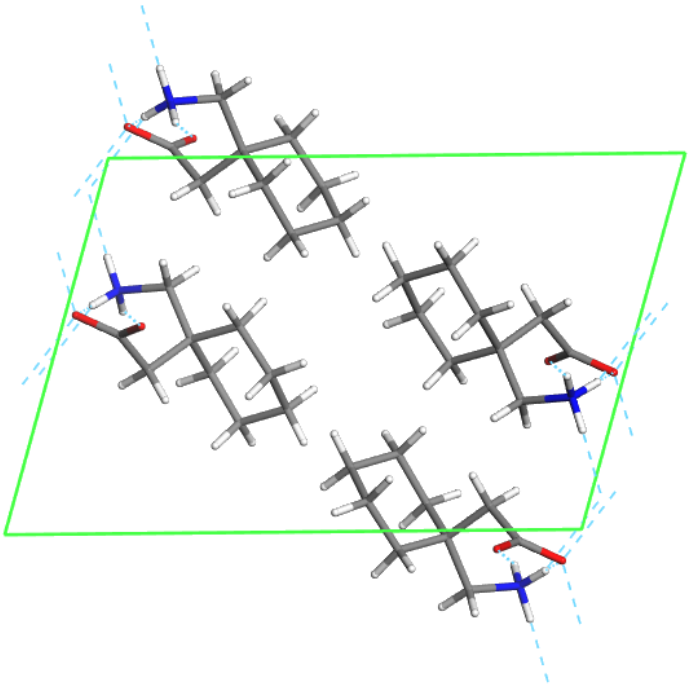

β-gabapentin

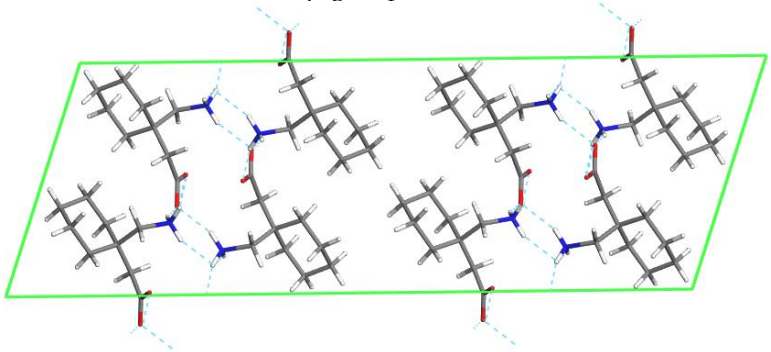

γ-gabapentin

Figure 3. Crystal structures of three known polymorphs of GBP.

The three GBP polymorphs were compared for their densities (1.257, 1.247, and 1.216 g cm^{-3}, respectively) and packing efficiencies (71.3, 70.5, and 68.7%, respectively), which revealed that α-gabapentin had the most efficiently packed molecules and was

therefore claimed the most thermodynamically stable form of anhydrous GBP. This thesis was additionally confirmed using DSC, which revealed that the order of stability is α > β > γ [31]. While the recrystallization of GBP in methanol always resulted in a pure α polymorph, it should be noted that when water was used for that purpose, monohydrate form I was the only one obtained (Figure 4) [32].

Slurry in methanol:

α → α γ → α γ + β → α

Slurry in water:

α → monohydrate form I
γ → monohydrate form I
γ + β → monohydrate form I

Figure 4. Slurry experiments.

Dehydration experiments of monohydrate form I showed that, depending on the experimental conditions, it results in either pure or mixed anhydrous phase mixtures (Figure 5).

100°C for 2 hours under vacuum	Monohydrate form I → α + γ + β
100°C for 30 minutes	Monohydrate form I → γ + β
dessicator with silica gel for 3 days	Monohydrate form I → β (not pure)
desiccator at 50°C for 3 days	Monohydrate form I → γ

Figure 5. Dehydration experiments.

Stability tests conducted under various humidity settings showed that form α maintained at 50% relative humidity (RH) remained stable, whereas form β and the combination of forms β and γ quantitatively changed into form α. Forms α, β, and the mixtures of forms β and γ all changed into monohydrate form I at 100% RH, which confirmed that the presence of water makes the monohydrate form I the most stable [32] (Figure 6).

50% RH:
α → α γ → α γ + β → α

100% RH:
α → monohydrate form I
γ → monohyrate form I
γ + β → monohydrate form I

Figure 6. Stability tests at 50% and 100% RH.

Grinding and kneading of forms β and γ, as well as their mixture, revealed complete conversion to form α after approximately 10 min of kneading (Figure 7). Form α does not change when it is ground, nor does it change after being recrystallized from a variety of solvents, including acetonitrile, chloroform, DMSO, methanol, hexane, and ethyl acetate. [32]. However, the crystallization outcomes of fast cooling crystallization were found to be dependent on supersaturation degree [54] (Figure 8).

Grinding and kneading:

$\alpha \rightarrow \alpha \qquad \gamma \rightarrow \alpha \qquad \gamma + \beta \rightarrow \alpha$

Kneading:

$\alpha \rightarrow \alpha$

Figure 7. Grinding and kneading experiments.

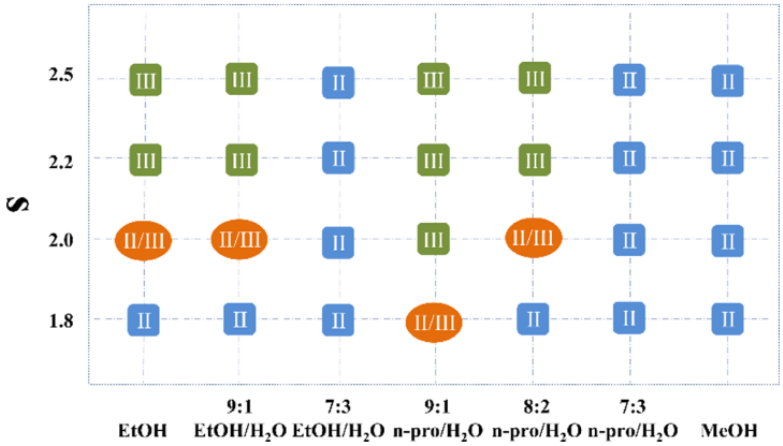

Figure 8. Polymorphic outcomes at different supersaturations (Ss) and solvents. I, II and III are the symbols of polymorphs of GBP. Adapted with permission from [54]. Copyright 2024 American Chemical Society.

5.2. Polymorhphism of GBP Monohydrate—Structures QIMKOMXX

In addition to anhydrous forms, GBP can also exist as various hydrates. So far, two polymorphs of GBP monohydrate have been described including polymorph I (QIMKOM, QIMKOM01, QIMKOM03) and polymorph II (QIMKOM02, QIMKOM04). In addition, GBP also occurs in the heptahydrate form as YUZTET (Table 3).

James A. Ibers, for the first time, obtained the monohydrate form I by dissolving GBP in water and then adding 2-propanol. The resulting solution was stored in a freezer. Four days later, crystals of GBP were extracted from a precipitate [28]. In another work [30], GBP monohydrate I crystals were harvested by the slow evaporation of a saturated ethanol–water solution at room temperature. The raw material used was gabapentin anhydrate form α. During single crystal examinations, multiple solvent amounts were used to ensure that either anhydrate form α or monohydrate exists steadily within the whole solvent composition range and that no other phase transformation occurs. The authors showed that anhydrate α was the more stable form at lower water percentages, and rising temperatures expanded the stability region. In contrast, monohydrate I was more stable at higher water percentages, but as the temperature rose, the stable area shrunk. Both solvent composition and temperature had a significant impact on the relative stability of GBP anhydrate α and monohydrate I. In the mentioned work, the authors used solvents of various alcohol/water ratios to obtain the intersections of the GBP anhydrate α and monohydrate I solubility curves, indicating the transition points. When the mole fraction of methanol in solvents increased from 10% to 30%, the transition temperature between the anhydrous and hydrate forms shifted from 308.56 K to 291.52 K. The transition temperature for an ethanol–water mixture containing 10% ethanol was approximately 314.44 K. When the ethanol level grew to 40%, the transition reduced to 293.80 K [30].

Pure monohydrate form II can be obtained, i.e., by grinding GBP with water and ethanol [34]; however, in some studies, monohydrate forms I and II have been obtained simultaneously. The distinctions between these two forms are minor and result from the development of primary aggregates into viable nuclei, which then propagate into single crystals [33].

In 2010, Fabbiani et al. [35], motivated by the rich structural variation in GBP observed at ambient pressure, performed high-pressure recrystallization of this compound. They found that GBP can exist in the form of a heptahydrate under increased pressure, starting from 0.8 GPa. To achieve this, a saturated aqueous gabapentin solution was inserted into the DAC under ambient pressure. The cell was sealed and gradually pressurized; at around 0.8 GPa, polycrystalline material precipitated. The temperature was then cycled around 313 K to dissolve all but one of the crystallites, and after cooling slowly to 293 K, a single crystal grew from the solution. The pressure at the end was 0.87 GPa. In a later recrystallization experiment, the authors were able to produce another single crystal (crystal B) in a very different manner from that previously achieved, as proved by comparing the orientation matrices determined on the same diffractometer. It was discovered that at the first growing stage, the crystal was relatively mobile, i.e., sensitive to DAC rotation, and could easily be displaced from the gasket edge through gentle warming. Although the rotation of the DAC allowed the crystal to move, this movement was uncontrollable; thus, the ultimate orientation of crystal B was attained by serendipity. The final pressure inside the DAC with crystal B was 0.9 GPa. Crystal B was grown under closely matched conditions to those for crystal A. The molecular conformation of GBP in the heptahydrate form was remarkably similar to that in the anhydrous β-form. The authors concluded that since GBP monohydrate did not crystallize during the high-pressure crystallization trials, the order of stability of anhydrous forms under high-pressure conditions may have changed.

6. Conformational Analysis of GBP in Solution

The conformational analysis of GBP has been the aim of several experimental and computational studies [55]. Bryans et al. demonstrated, utilizing low-temperature ^{1}H NMR techniques, that at −80 °C, two sets of exocyclic methylene signals were observed at a ratio of 1:2. These signals corresponded to the two conformers of GBP, with the aminomethyl moiety located either axial (**AX**, less abundant) or equatorial (**EQ**, more abundant), respectively, as shown in Figure 9. The same authors analyzed GBP by ^{1}H NMR in deuteromethanol at room temperature, where only a single set of signals was observed, owing to the rapid ring flipping at this temperature. Ananda et al. [29], by recording ^{1}H NMR spectra at −86 °C in deuterated methanol, determined the population ratio for the **AX/EQ** as 0.27:0.73 and the free energy difference, ΔG, between those two forms as 0.38 kcal mol^{-1}.

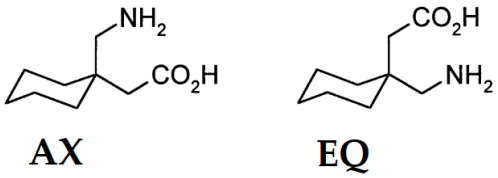

Figure 9. Two conformations of GBP, with the aminomethyl moiety located either in the axial (**AX**) or equatorial (**EQ**) position.

In a recent study [45], Liu et al. explored the conformational space of GBP in a more detailed way, using quantum mechanical calculations and molecular dynamics simulations. To achieve this aim, they extracted conformations II, III, and IV from their corresponding unit cells (of forms α-II, β-IV, and γ-III, respectively). According to the computational results, the order of stability of conformers (IV > III > II) was totally opposite to their corresponding polymorphs (II > III > IV). However, this was in accordance with the previously described NMR results, as conformer IV could be classified as **EQ,** while conformers III and II could be classified as **AX**. In addition, the authors identified the conformer present in the global minimum and named it conformer VI (Figure 10).

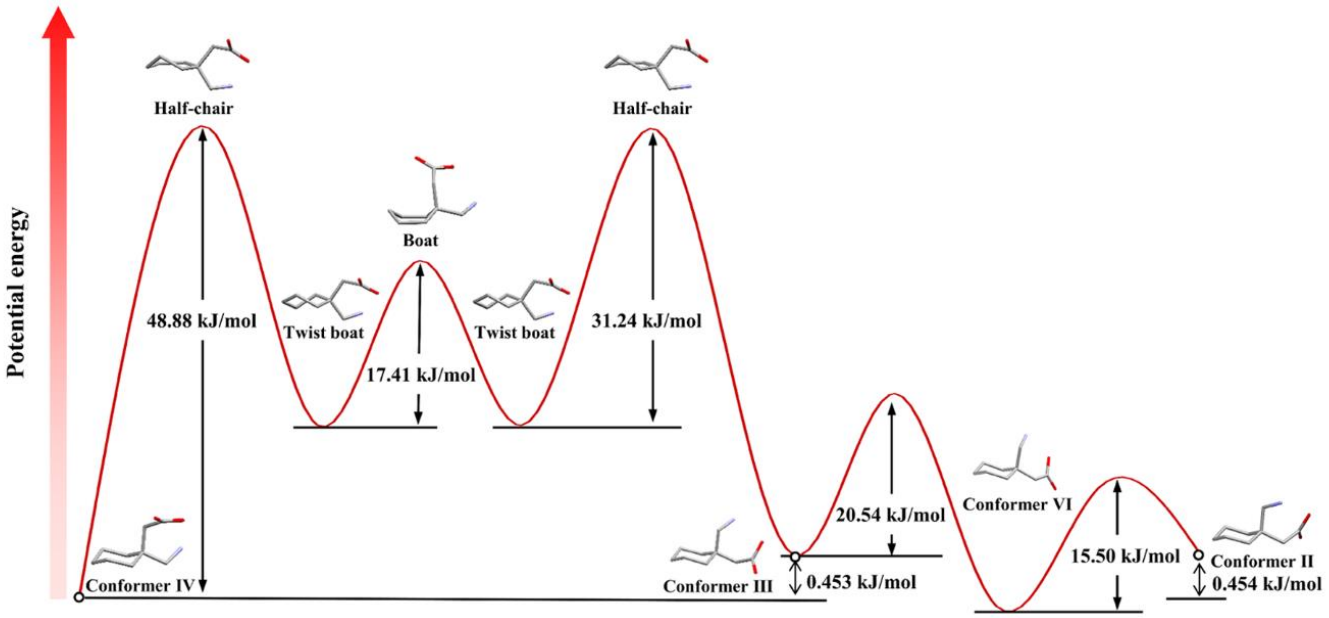

Figure 10. Transformation among conformers in methanol based on the conformational energy of conformer IV. Adapted with permission from [54]. Copyright 2024 American Chemical Society.

7. Conformational Analysis of GBP in a Solid State

Table 4 presents the chosen structural parameters of the GBP molecules extracted from their crystal structures.

Table 4. Chosen structural parameters of the GBP molecules extracted from their crystal structures. Structures are presented in the alphabetical order of their refcodes. To facilitate the analysis of the data, a 3-color scale was applied to compare the bond lengths. In this scale, the 50th percentile (midpoint) was calculated, and the cell that holds this value was colored yellow. The cells that hold the minimum value were colored green, and the cells that hold the maximum values were colored red.

Refcode	Ionization	Bond Lengths [Å]			Puckering Parameters		CH_2NH_2 Position
		C-N	C-O*	C-O**	Θ [°]	Q [Å]	
ANISAS	ZI	1.4868	1.2576	1.2577	176.540	0.558	AX
ANISAS *	ZI	1.5035	1.2643	1.2625	4.859	0.552	AX
ANISEW	ZI	1.4500	1.2560	1.2445	140.528	0.670	AX
ANISEW *	ZI	1.4927	1.2288	1.2326	177.246	0.554	EQ
ANISEW **	ZI	1.5001	1.2445	1.2746	177.950	0.551	EQ
ANISEW ***	ZI	1.2746	1.2635	1.2308	12.361	0.580	AX
AVAVAV	cation	1.4948	1.3141	1.2200	178.679	0.558	EQ
AVILOH	cation	1.4959	1.3167	1.2226	178.345	0.552	EQ
AVILUN	ZI	1.4867	1.2383	1.2867	177.094	0.554	EQ
AWUWIY	cation	1.4822	1.3164	1.2012	178.293	0.548	EQ
AWUWIY01	cation	1.4875	1.3274	1.2105	178.258	0.554	EQ
AWUWIY02	cation	1.4986	1.3182	1.1957	179.201	0.533	EQ
DESNOI	ZI	1.4946	1.2627	1.2552	176.808	0.559	EQ
DOBBIG	ZI	1.4884	1.2799	1.2427	174.637	0.566	EQ
DOBBIG2	ZI	1.4796	1.2823	1.2229	2.219	0.550	AX
DOBBOM	ZI	1.4706	1.2889	1.2349	177.149	0.543	EQ
DOBBOM2	ZI	1.4706	1.2889	1.2349	177.100	0.543	EQ
EFIVIB	ZI	1.4846	1.2818	1.2456	173.788	0.550	EQ
ELUNOP	ZI	1.4979	1.2519	1.2380	176.896	0.569	EQ
FOXNOW	ZI	1.4958	1.2659	1.2575	174.871	0.558	EQ

Table 4. *Cont.*

Refcode	Ionization	Bond Lengths [Å]			Puckering Parameters		CH_2NH_2 Position
		C-N	C-O*	C-O**	Θ [°]	Q [Å]	
FOXNUC	cation	1.4916	1.2803	1.2451	175.027	0.560	EQ
FOXNUC *	cation	1.4916	1.2803	1.2451	174.99	0.561	EQ
FOXPAK	cation	1.4953	1.3290	1.2103	175.327	0.560	EQ
FOXPAK *	cation	1.4942	1.3279	1.2099	5.628	0.559	AX
FOXPEO	cation	1.4886	1.3013	1.2189	2.754	0.557	AX
FOXPOY	cation	1.4863	1.3289	1.2116	178.246	0.557	EQ
IKATIY	cation	1.4837	1.3131	1.2131	2.010	0.559	AX
JALXAY	ZI	1.4809	1.2603	1.2481	178.968	0.550	EQ
JALXAY *	ZI	1.4737	1.2500	1.2623	178.26	0.537	EQ
JALXAY **	ZI	1.4924	1.2705	1.2372	1.58	0.535	AX
JALXAY ***	ZI	1.4954	1.2691	1.2325	2.302	0.544	AX
JALXEC	ZI	1.4966	1.2804	1.2522	176.202	0.550	EQ
JALXEC *	ZI	1.4952	1.2851	1.2460	176.013	0.545	EQ
LORQIT	cation	1.4968	1.3147	1.2171	176.816	0.550	EQ
NUPXAY	cation	1.4761	1.3099	1.2135	2.498	0.554	AX
QIMKIG	ZI	1.4999	1.2716	1.2522	5.054	0.551	AX
QIMKIG01	ZI	1.4995	1.2677	1.2405	4.736	0.551	AX
QIMKIG02	ZI	1.4860	1.2657	1.2409	176.491	0.560	EQ
QIMKIG03	ZI	1.4836	1.2633	1.2440	2.444	0.552	AX
QIMKIG04	ZI	1.4859	1.2619	1.2450	177.559	0.554	EQ
QIMKIG05	ZI	1.4887	1.2629	1.2504	2.451	0.556	AX
QIMKIG06	ZI	1.4993	1.2653	1.2458	4.719	0.550	AX
QIMKOM	ZI	1.4923	1.2680	1.2514	3.070	0.556	AX
QIMKOM01	ZI	1.4907	1.2630	1.2486	3.168	0.555	AX
QIMKOM02	ZI	1.4865	1.2647	1.2507	3.082	0.551	AX
QIMKOM03	ZI	1.4904	1.2599	1.2450	3.304	0.549	AX
QIMKOM04	ZI	1.4862	1.2582	1.2539	3.240	0.562	AX
SESKEI	ZI	1.5036	1.2752	1.2671	174.05	0.573	EQ
SESKEI *	ZI	1.4887	1.2759	1.2723	177.625	0.54	EQ
SOCYUF	cation	1.4927	1.3154	1.2161	1.382	0.558	AX
UQUMOJ	ZI	1.4899	1.2608	1.2603	179.039	0.559	EQ
UQUMOJ *	ZI	1.4899	1.2608	1.2603	179.001	0.559	EQ
UQUMOJ **	ZI	1.4849	1.2576	1.2526	2.610	0.553	AX
UQUMOJ ***	ZI	1.4849	1.2576	1.2526	2.626	0.553	AX
VIXBUB	ZI	1.5026	1.2668	1.2595	178.013	0.546	EQ
VIXBUB *	ZI	1.5099	1.2790	1.2526	2.728	0.560	AX
VIXBUB **	ZI	1.4960	1.2690	1.2529	4.688	0.552	AX
VIXBUB ***	ZI	1.5026	1.2668	1.2595	178.013	0.546	EQ
VIXBUB ****	ZI	1.5099	1.2790	1.2526	2.728	0.560	AX
VIXBUB *****	ZI	1.4960	1.2690	1.2529	4.688	0.552	AX
VIXCAI	ZI	1.4912	1.2597	1.2534	1.588	0.553	AX
VIXCAI *	ZI	1.4912	1.2597	1.2534	1.650	0.552	AX
VIXCAI **	ZI	1.5237	1.2662	1.2459	4.233	0.561	AX
VIXCAI ***	ZI	1.5237	1.2662	1.2459	4.235	0.561	AX
VIXCAI ****	ZI	1.5017	1.2792	1.2381	2000	0.543	AX
VIXCAI *****	ZI	1.4733	1.2658	1.2450	3.103	0.559	AX
VIXCAI ******	ZI	1.5246	1.2680	1.2490	2.558	0.550	AX
VIXCAI *******	ZI	1.5246	1.2680	1.2490	2.625	0.550	AX
VIXCAI ********	ZI	1.4733	1.2658	1.2450	3.045	0.559	AX
VIXCAI *********	ZI	1.5017	1.2792	1.2381	1.962	0.544	AX
VIXCEM	ZI	1.4942	1.2662	1.2569	177.542	0.553	EQ
VIXCEM *	ZI	1.4935	1.2696	1.2318	177.542	0.553	AX
VIXCEM01	ZI	1.4939	1.2777	1.2418	3.161	0.547	EQ
VIXCEM01 *	ZI	1.4942	1.2662	1.2569	2.276	0.538	AX
VIXCIQ	ZI	1.4903	1.2851	1.2255	3.090	0.556	AX
VIXCIQ *	ZI	1.4903	1.2851	1.2255	3.004	0.556	AX

Table 4. *Cont.*

Refcode	Ionization	Bond Lengths [Å]			Puckering Parameters		CH_2NH_2 Position
		C-N	C-O*	C-O**	Θ [°]	Q [Å]	
VIXCIQ ***	ZI	1.5012	1.2739	1.2510	175.306	0.537	EQ
VIXCIQ ****	ZI	1.5012	1.2739	1.2510	175.329	0.537	EQ
VIXCUC	ZI	1.5151	1.2854	1.2538	3.097	0.551	AX
VIXCUC *	ZI	1.5151	1.2854	1.2538	3.097	0.551	AX
VIXCUC **	ZI	1.5136	1.2721	1.2512	3.708	0.556	AX
VIXCUC ***	ZI	1.5035	1.2723	1.2577	178.596	0.557	EQ
VIXCUC ****	ZI	1.5035	1.2723	1.2577	178.596	0.557	EQ
VIXCUC *****	ZI	1.5136	1.2721	1.2512	3.708	0.556	AX
VIXDAJ	ZI	1.4955	1.2703	1.2603	2.886	0.576	AX
VIXDAJ *	ZI	1.4831	1.2623	1.2558	177.366	0.560	EQ
VIXDAJ **	ZI	1.5026	1.2591	1.2530	3.655	0.561	AX
VIXDAJ ***	ZI	1.4955	1.2703	1.2603	2.886	0.576	AX
VIXDAJ ****	ZI	1.4831	1.2623	1.2558	177.366	0.560	EQ
VIXDAJ *****	ZI	1.5026	1.2591	1.2530	3.655	0.561	AX
VIXDEN	ZI	1.4969	1.2808	1.2669	1.425	0.523	AX
VIXDEN *	ZI	1.5099	1.2545	1.2459	3.392	0.541	AX
VIXDEN **	ZI	1.4696	1.2780	1.2735	1.068	0.555	AX
VIXDEN ***	ZI	1.5085	1.2777	1.2535	175.266	0.562	EQ
VIXDEN ****	ZI	1.4907	1.2592	1.2504	2.758	0.538	AX
VIXDEN *****	ZI	1.4868	1.2551	1.2482	178.287	0.548	EQ
VIXDEN ******	ZI	1.5360	1.2633	1.2406	1.092	0.560	AX
VIXDEN *******	ZI	1.5009	1.2685	1.2618	175.248	0.555	EQ
VIXQAW	ZI	1.4846	1.2798	1.2531	165.087	0.502	EQ
VIXQAW1*	ZI	1.5082	1.2594	1.2455	1.119	0.546	EQ
VIXQAW **	ZI	1.4846	1.2798	1.2531	165.042	0.502	AX
VIXQAW ***	ZI	1.4767	1.2714	1.2353	2.893	0.545	EQ
VIXQAW ****	ZI	1.5188	1.2885	1.2484	175.464	0.560	AX
VIXQAW *****	ZI	1.5079	1.2646	1.2602	1.962	0.554	AX
VIXQAW ******	ZI	1.4767	1.2714	1.2353	2.908	0.545	AX
VIXQAW *******	ZI	1.5188	1.2885	1.2484	175.504	0.561	AX
VIXQAW ********	ZI	1.3978	1.2639	1.2477	177.357	0.575	AX
VIXQAW *********	ZI	1.5002	1.2664	1.2502	2.227	0.555	AX
VIXQAW **********	ZI	1.3978	1.2639	1.2477	177.363	0.575	EQ
VIXQAW **********	ZI	1.5002	1.2664	1.2502	2.309	0.554	AX
VIXQAW ***********	ZI	1.5573	1.2680	1.2494	2.179	0.537	EQ
VIXQAW ************	ZI	1.5573	1.2680	1.2494	2.176	0.536	AX
VIXQAW *************	ZI	1.5082	1.2594	1.2455	1.147	0.546	AX
VIXQAW **************	ZI	1.5079	1.2646	1.2602	1.993	0.554	EQ
VIXQEA	ZI	1.5125	1.2583	1.2525	3.323	0.552	AX
VIXQEA *	ZI	1.4637	1.2710	1.2577	3.144	0.543	AX
VIXQEA **	ZI	1.5206	1.2656	1.2646	3.821	0.553	AX
VIXQEA ***	ZI	1.5206	1.2656	1.2646	3.826	0.553	AX
VIXQEA ****	ZI	1.5125	1.2583	1.2525	3.323	0.552	AX
VIXQEA *****	ZI	1.5050	1.2728	1.2506	6.086	0.515	AX
VIXQEA ******	ZI	1.4637	1.2710	1.2577	3.156	0.543	AX
VIXQEA *******	ZI	1.5088	1.2544	1.2483	2.799	0.553	AX
VIXQEA ********	ZI	1.5050	1.2728	1.2506	6.084	0.516	AX

Table 4. *Cont.*

Refcode	Ionization	Bond Lengths [Å]			Puckering Parameters		CH_2NH_2 Position
		C-N	C-O*	C-O**	Θ [°]	Q [Å]	
VIXQEA ********	ZI	1.5088	1.2544	1.2483	2.797	0.553	AX
YUZTET	ZI	1.4922	1.2584	1.2529	176.962	0.547	EQ
Average		1.4932	1.2731	1.2464		0.553	
Standard deviation		0.0282	0.0184	0.0153		0.016	

For structures with Z′ > 1, asterisks (*) are used to distinguish the nonequivalent conformations; **ZI**—zwitterion; **CO***—for cations, this is the length of the single bond, and for zwitterions, this is the length of the longer of two C-O bonds; **CO****—for cations, this is the length of the double bond, and for zwitterions, this is the length of the shorter of two C-O bonds; **AX**—the aminomethyl moiety is located axially; **EQ**—the aminomethyl moiety located equatorially.

An analysis of the values presented in Table 4 reveals a wide range of C-N bond lengths of GBP in the crystal structures that contain this API, from 1.2746 to 1.5573 Å. While a lower value is typical for C=N bonds, such as those in imines, the 1.5573 Å value looks suspicious as the longest C-N bonds rarely exceed 1.53 Å.

In most cases, the ionization state of GBP can be easily determined based on the differences between the CO* and CO** lengths, which are similar in zwitterions and diverse in cations. The sole exception here is the FOXNUC structure, which was already described in detail and presented in Figure 2. In most of the analyzed conformations, GBP exists as zwitterion (89%), and in the rest, it forms a cation. So far, the crystal structure of a compound in which GBP exists as an anion has not been determined.

In most cases (60%), GBP exists in the **AX** conformation, including the thermodynamically most stable polymorph α (II). However, it has been shown in both experimental and computational studies, as described above, that **EQ** is the more stable conformation in solution. As in the crystals with Z′ > 1, both **AX** and **EQ** conformers can be found within the same unit, which shows that the intermolecular forces play a major role in the stabilization of the chosen system rather than the intramolecular energy of a particular conformer.

An analysis of the puckering parameters revealed that in most cases, θ was either $0 \pm 5°$ or $180 \pm 5°$, which indicates the chair, ***C***, conformation of the substituted cyclohexane ring as either $^4C_1$ or $^1C_4$, respectively. The average total puckering amplitude, Q, was found to be 0.553 ± 0.016 Å, which lies only slightly under the Q value of glucopyranose (0.560 Å) and an ideal cyclohexane chair (0.630 Å). The most distinct values of the puckering parameters were calculated for two different conformations in ANISEW, namely, ANISEW and ANISEW**, with θ and Q values of 140.528°, 0.670 Å and 12.361°, 0.580 Å, respectively. Such values of θ indicate a great distortion from **C**, especially for ANISEW (Figure 11). Taking into account that in ANISEW*** and ANISEW*, respectively, the shortest C-N (1.2746 Å) and C-O* (1.2326 Å) bond lengths were observed, this may indicate that this structure should be revisited.

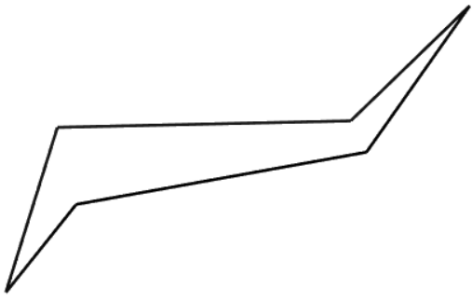

Figure 11. Cyclohexane ring of ANISEW *** showing distortion from the chair conformation.

8. Conclusions

Gabapentin is an important API, with a complex mechanism of action and broad therapeutical applications. Due to its pharmacokinetic properties, leading to the necessity of frequent drug administration, multiple crystal structures containing GBP have been successfully obtained and analyzed. Moreover, GBP is a versatile building block in crystal engineering. Being a Lewis base, GBP has been used multiple times as a ligand to create various complexes. Also, due to the presence of H bond donors and acceptors in GBP molecules, multiple schemes of the H bonding network can be observed in GBP-related structures. GBP exhibits polymorphism both in its anhydrous and monohydrate forms, with the α (II) anhydrate and monohydrate I forms being the thermodynamically most stable ones. However, results of recent high-pressure crystallization studies and quantum chemical calculations indicate that the entire landscape of GBP has not been revealed yet.

This review can serve as a starting point for new structural studies of GBP and related compounds. First, it is advisable to perform polymorphic screening under higher pressure, as this can be the source of new forms that have not been discovered yet. In addition, the quantum mechanics calculation studies that have already started can be further continued to reveal other possible polymorphs of GBP and the conditions required to obtain them.

Author Contributions: Conceptualization, Ł.S.; methodology, Ł.S.; formal analysis, Ł.S.; investigation, J.B. and Ł.S.; data curation, J.B. and Ł.S.; writing—original draft preparation, J.B. and Ł.S.; writing—review and editing, J.B. and Ł.S.; visualization, J.B. and Ł.S.; supervision, Ł.S.; project administration, Ł.S.; funding acquisition, Ł.S. All authors have read and agreed to the published version of the manuscript.

Funding: This research received no external funding.

Data Availability Statement: The data presented in this study are available on request from the corresponding author.

Conflicts of Interest: The authors declare no conflicts of interest.

References

1. Herbst, M.; Komisarek, D.; Strothmann, T.; Vasylyeva, V. A Lection in Humbleness: Crystallization of Chiral and Zwitterionic APIs Baclofen and Phenibut. *Crystals* **2022**, *12*, 1393. [CrossRef]
2. Refat, M.S.; Hamza, R.Z.; Adam, A.M.A.; Saad, H.A.; Gobouri, A.A.; Al-Salmi, F.A.; Altalhi, T.A.; El-Megharbel, S.M. Potential Therapeutic Effects of New Ruthenium (III) Complex with Quercetin: Characterization, Structure, Gene Regulation, and Antitumor and Anti-Inflammatory Studies (RuIII/Q Novel Complex Is a Potent Immunoprotective Agent). *Crystals* **2021**, *11*, 367. [CrossRef]
3. Udaykumar Rao, B.; Maqdoom, F.; Nikalje, A.P. Determination of gabapentin in bulk drug and in pharmaceutical dosage form by HPLC method. *J. Chil. Chem. Soc.* **2009**, *54*, 424–427. [CrossRef]
4. Rose, M.A.; Kam, P.C. Gabapentin: Pharmacology and its use in pain management. *Anaesthesia* **2002**, *57*, 451–462. [CrossRef]
5. Calandre, E.P.; Rico-Villademoros, F.; Slim, M. Alpha2delta ligands, gabapentin, pregabalin and mirogabalin: A review of their clinical pharmacology and therapeutic use. *Expert Rev. Neurother.* **2016**, *16*, 1263–1277. [CrossRef]
6. Duncan, J.S.; Sander, J.W.; Sisodiya, S.M.; Walker, M.C. Adult epilepsy. *Lancet* **2006**, *367*, 1087–1100. [CrossRef]
7. Asadi-Pooya, A.A.; Brigo, F.; Lattanzi, S.; Blumcke, I. Adult epilepsy. *Lancet* **2023**, *402*, 412–424. [CrossRef]
8. Bruno, I.J.; Cole, J.C.; Edginton, P.R.; Kessler, M.; Macrae, C.F.; Mccabe, P.; Pearson, J.; Taylor, R. New software for searching the Cambridge Structural Database and visualizing crystal structures. *Acta Cryst.* **2002**, *B58*, 389–397. [CrossRef]
9. CCDC Search Structures Application. Available online: https://www.ccdc.cam.ac.uk/structures/ (accessed on 22 January 2024).
10. Model the Biosphere | BIOVIA—Dassault Systèmes. Available online: https://www.3ds.com/products-services/biovia/ (accessed on 22 January 2024).
11. Cremer-Pople Parameter Calculator. Available online: http://enzyme13.bt.a.u-tokyo.ac.jp/CP/ (accessed on 22 January 2024).
12. Chincholkar, M. Gabapentinoids: Pharmacokinetics, pharmacodynamic and considerations for clinical practice. *Br. J. Pain* **2020**, *14*, 104–114. [CrossRef] [PubMed]
13. Smith, R.V.; Havens, J.R.; Walsh, S.L. Gabapentin misuse, abuse and diversion: A systematic review. *Addiction* **2016**, *111*, 1160–1174. [CrossRef] [PubMed]
14. Maneuf, Y.P.; Luo, Z.D.; Lee, K. α2δ and the mechanism of action of gabapentin in the treatment of pain. *Semin. Cell Dev. Biol.* **2006**, *17*, 565–570. [CrossRef]
15. Bockbrader, H.N.; Wesche, D.; Miller, R.; Chapel, S.; Janiczek, N.; Burger, P. A Comparison of the Pharmacokinetics and Pharmacodynamics of Pregabalin and Gabapentin. *Clin. Pharmacokinet* **2010**, *49*, 661–669. [CrossRef]

16. Jackson, C.; Clanahan, M.J.; Joglekar, K.; Decha-Umphai, S.T. Hold the gaba: A case of gabapentin-induced hepatotoxicity. *Cureus* **2018**, *10*, e2269. [CrossRef]
17. Hakami, T. Neuropharmacology of Antiseizure Drugs. *Neuropsychopharmacol. Rep.* **2021**, *41*, 336–351. [CrossRef]
18. Minozzi, S.; Cinquini, M.; Amato, L.; Farrell, M.F.; Reisser, A.A.R.L.; Pani, P.P.; de Lima, M.S.; Soares, B.G.O.; Vecchi, S. Anticonvulsants for cocaine dependence. *Cochrane Database Syst. Rev.* **2015**, *2015*, CD006754. [CrossRef] [PubMed]
19. Marschall, K.; Gowing, L.; Ali, R.; Le Foll, B. Pharmacotherapies for cannabis dependence. *Cochrane Database Syst. Rev.* **2014**, *12*, CD008940. [CrossRef] [PubMed]
20. Pani, P.P.; Trogu, E.; Pacini, M.; Maremmani, I. Anticonvulsants for alcohol dependence. *Cochrane Database Syst. Rev.* **2014**, *2014*, CD008544. [CrossRef]
21. Hornyak, M.; Scholz, H.; Kohnen, R.; Bengel, J.; Kassubek, J.; Trenkwalder, C. What treatment works best for restless legs syndrome? Meta-analyses of dopaminergic and non-dopaminergic medications. *Sleep Med. Rev.* **2014**, *18*, 153–164. [CrossRef]
22. Aurora, R.N.; Kristo, D.A. The treatment of restless legs syndrome and periodic limb movement disorder in adults—An update for 2012: Practice parameters with an evidence-based systematic review and meta-analyses: An American Academy of Sleep Medicine Clinical Practice Guideline. *Sleep* **2012**, *35*, 1039–1062. [CrossRef]
23. Tozihi, M.; Bahrami, H.; Zarifian, M.; Vahedpour, M. Protonation of gabapentin: Ion mobility spectrometry and computational study. *Eur. J. Mass Spectrom.* **2023**, *29*, 220–230. [CrossRef]
24. Morozov, Y.N.; Mikhalev, S.P.; Shabatin, V.P.; Kolotilov, P.N.; Sergeev, G.B. Cryomodification of drugs: Micronization and crystalline structures of 1-(aminomethyl)-cyclohexaneacetic acid. *Mosc. Univ. Chem. Bull.* **2010**, *65*, 237–243. [CrossRef]
25. Sinha, L.; Karabacak, M.; Narayan, V.; Cinar, M.; Prasad, O. Molecular structure, electronic properties, NLO, NBO analysis and spectroscopic characterization of Gabapentin with experimental (FT-IR and FT-Raman) techniques and quantum chemical calculations. *Spectrochim. Acta Part A Mol. Biomol. Spectrosc.* **2013**, *109*, 298–307. [CrossRef]
26. Mahmoud, M.A.; Abbas, A.M.; Zaitone, S.A.; Ammar, A.M.; Sallam, S.A. Copper (II) ternary complexes with gabapentin and neurotransmitters as antiepileptic drug. *J. Mol. Struct.* **2019**, *1180*, 861–877. [CrossRef]
27. Mahmoud, M.A.; Helal, M.A.; Ammar, A.M. Zinc ternary complexes with gabapentin and neurotransmitters: Synthesis, spectral, thermal and molecular docking studies. *J. Mol. Struct.* **2020**, *1199*, 126951. [CrossRef]
28. Ibers, J.A. Gabapentin and gabapentin monohydrate. *Acta Crystallogr. C* **2001**, *57*, 641–643. [CrossRef]
29. Ananda, K.; Aravinda, S.; Vasudev, P.G.; Raja, K.M.P.; Sivaramakrishnan, H.; Nagarajan, K.; Shamala, N.; Balaram, P. Stereochemistry of gabapentin and several derivatives: Solid state conformations and solution equilibria. *Curr. Sci.* **2003**, *85*, 1002–1011.
30. Wang, Y.; Du, S.; Wu, S.; Zhang, D.; Yu, B.; Bekele, H.K.; Gong, J. Thermodynamic and molecular investigation into the solubility, stability and self-assembly of gabapentin anhydrate and hydrate. *J. Chem. Thermodyn.* **2017**, *113*, 132–143. [CrossRef]
31. Reece, H.A.; Levendis, D.C. Polymorphs of gabapentin. *Acta Crystallogr C* **2008**, *64*, 105–108. [CrossRef]
32. Braga, D.; Grepioni, F.; Maini, L.; Rubini, K.; Polito, M.; Brescello, R.; Cotarca, L.; Duarte, M.T.; Andre, V.; Fatima, M.; et al. Polymorphic gabapentin: Thermal behaviour, reactivity and interconversion of forms in solution and solid-state. *New J. Chem.* **2008**, *32*, 1788–1795. [CrossRef]
33. Vasudev, P.G.; Aravinda, S.; Ananda, K.; Veena, S.D.; Nagarajan, K.; Shamala, N.; Balaram, P. Crystal Structures of a New Polymorphic Form of Gabapentin Monohydrate and the E and Z Isomers of 4-Tertiarybutylgabapentin. *Chem. Biol. Drug Des.* **2009**, *73*, 83–96. [CrossRef]
34. Zhao, C.; Su, X.; Fang, L.; Shang, Z.; Li, Z.; Gong, J.; Wu, S. Multivariate Analysis of a Highly Effective Drug Combination Tablet Containing the Antiepileptic Drug Gabapentin to Enhance Pharmaceutical Properties with a Multicomponent Crystal Strategy. *Cryst. Growth Des.* **2022**, *12*, 7234–7247. [CrossRef]
35. Fabbiani, F.P.A.; Levendis, D.C.; Buth, G.; Kuhs, W.F.; Shankland, N.; Sowa, H. Searching for novel crystal forms by in situ high-pressure crystallisation: The example of gabapentin heptahydrate. *CrystEngComm* **2010**, *12*, 2354–2360. [CrossRef]
36. Jasinski, J.P.; Butcher, R.J.; Yathirajan, H.S.; Mallesha, L.; Mohana, K.N.; Narayana, B. Crystal Structure of a Second Polymorph of Gabapentin Hydrochloride Hemihydrate with a Three-Center Bifurcated Hydrogen Bond. *J. Chem. Crystallogr.* **2009**, *39*, 777–780. [CrossRef]
37. André, V.; Marques, M.M.; da Piedade, M.F.M.; Duarte, M.T. An ester derivative of the drug gabapentin: pH dependent crystal stability. *J. Mol. Struct.* **2010**, *973*, 173–179. [CrossRef]
38. André, V.; Fernandes, A.; Santos, P.P.; Duarte, M.T. On the Track of New Multicomponent Gabapentin Crystal Forms: Synthon Competition and pH Stability. *Cryst. Growth Des.* **2011**, *11*, 2325–2334. [CrossRef]
39. Wenger, M.; Bernstein, J. An Alternate Crystal Form of Gabapentin: A Cocrystal with Oxalic Acid. *Cryst. Growth Des.* **2008**, *8*, 1595–1598. [CrossRef]
40. Hongqi, L.; Yathirajan, H.S.; Mellesha, L.; Mohana, K.N.; Narayana, B. Gabapentinium picrate. *Acta Cryst. E* **2009**, *65*, 783.
41. Shaikjee, A.; Levendis, D.C.; Marques, H.M.; Mampa, R. A gold(III) complex and a tetrachloroaurate salt of the neuroepileptic drug gabapentin. *Inorg. Chem. Commun.* **2011**, *14*, 534–538. [CrossRef]
42. Reddy, L.; Bethune, S.J.; Kampf, J.W.; Rodríguez-Hornedo, N. Cocrystals and Salts of Gabapentin: pH Dependent Cocrystal Stability and Solubility. *Cryst. Growth Des.* **2009**, *9*, 378–385. [CrossRef]
43. Vries, E.J.C.; Gamble, C.; Shaikjee, A. [1-(Carboxymethyl)cyclohexyl]- methanaminium nitrate. *Acta Cryst. E* **2011**, *67*, 513. [CrossRef]

44. Razzaq, S.N.; Khan, I.U.; Şahin, O.; Büyükgüngör, O. [1-(Carboxymethyl)cyclohexyl]methanaminium dihydrogen phosphate. *Acta Cryst. E* **2010**, *66*, 1074. [CrossRef]
45. Fowler, D.A.; Tian, J.; Barnes, C.; Teat, S.J.; Atwood, J.L. Cocrystallization of C-butyl pyrogallol[4]arene and C-propan-3-ol pyrogallol[4]arene with gabapentin. *CrystEngComm* **2011**, *13*, 1446–1449. [CrossRef]
46. Spiel, P.D.; Sikligar, K.; Baker, G.A.; Kelley, S.P.; Atwood, J.L. Cocrystallization of C-Propyl Pyrogallol[4]arene and the Pharmaceutical Gabapentin. *J Chem. Crystallogr.* **2018**, *49*, 119–124. [CrossRef]
47. Kumari, H.; Zhang, J.; Erra, L.; Barbour, L.J.; Deakyne, C.A.; Atwood, J.L. Cocrystals of gabapentin with C-alkylresorcin[4]arenes. *CrystEngComm* **2013**, *15*, 4045. [CrossRef]
48. Queresma, S.; André, V.; Antunes, A.M.M.; Cunha-Silva, L.; Duarte, M.T. Gabapentin Coordination Networks: Mechanochemical Synthesis and Behavior under Shelf Conditions. *Cryst. Growth Des.* **2013**, *13*, 5007–5017. [CrossRef]
49. Vries, E.J.C.; Gamble, C.; Shaikjee, A. Tetraaquatetrakis{μ_2-[1-(carboxylatomethyl)cyclohexyl]methanaminium}-bis(μ_3-hydroxido)bis(nitrato-κ^2O,O′)-tetrazinc(II). *Acta Cryst. E* **2011**, *67*, 573–574. [CrossRef] [PubMed]
50. Braga, D.; Grepioni, F.; Maini, L.; Brescello, R.; Cotarca, L. Simple and quantitative mechanochemical preparation of the first zinc and copper complexes of the neuroleptic drug gabapentin. *CrystEngComm* **2008**, *10*, 469–471. [CrossRef]
51. Mungalimane, A.; Shetty, V. CCDC 982169: Experimental Crystal Structure Determination, 2017. Available online: https://www.ccdc.cam.ac.uk/structures/ (accessed on 22 January 2024).
52. Pesachovich, M.; Singer, C.; Pilarski, G. Preparation of Gabapentin. U.S. Patent No. 6,255,526,B1, 2 July 2001.
53. Satyanarayana, C.; Ramanjaneyulu, G.S.; Kumar, I.V.S. *World Intellectual Property Organization, Publication No. WO 2004/110342*; WIPO: Karlsruhe, Germany, 2004.
54. Liu, Y.; Wang, Y.; Huang, X.; Li, X.; Zong, S.; Wang, N.; Hao, H. Conformational Selectivity and Evolution Affected by the Desolvation Process. *Cryst. Growth Des.* **2022**, *22*, 1283–1291. [CrossRef]
55. Bryans, J.S.; Horwell, D.C.; Ratcliffe, G.S.; Recevaur, J.M.; Rubin, J.R. An In Vitro Investigation into Conformational Aspects of Gabapentin. *Bioorg. Med. Chem.* **1999**, *8*, 715–721. [CrossRef]